Establishment of 5′–3′ interactions in mRNA independent of a continuous ribose-phosphate backbone

FLORIAN KLUGE, MICHAEL GÖTZE,[1] and ELMAR WAHLE

Institute of Biochemistry and Biotechnology and Charles Tanford Protein Center, Martin Luther University Halle-Wittenberg, 06099 Halle, Germany

ABSTRACT

Functions of eukaryotic mRNAs are characterized by intramolecular interactions between their ends. We have addressed the question whether 5′ and 3′ ends meet by diffusion-controlled encounter "through solution" or by a mechanism involving the RNA backbone. For this purpose, we used a translation system derived from *Drosophila* embryos that displays two types of 5′–3′ interactions: Cap-dependent translation initiation is stimulated by the poly(A) tail and inhibited by Smaug recognition elements (SREs) in the 3′ UTR. Chimeric RNAs were made consisting of one RNA molecule carrying a luciferase coding sequence and a second molecule containing SREs and a poly(A) tail; the two were connected via a protein linker. The poly(A) tail stimulated translation of such chimeras even when disruption of the RNA backbone was combined with an inversion of the 5′–3′ polarity between the open reading frame and poly(A) segment. Stimulation by the poly(A) tail also decreased with increasing RNA length. Both observations suggest that contacts between the poly(A) tail and the 5′ end are established through solution, independently of the RNA backbone. In the same chimeric constructs, SRE-dependent inhibition of translation was also insensitive to disruption of the RNA backbone. Thus, tracking of the backbone is not involved in the repression of cap-dependent initiation. However, SRE-dependent repression was insensitive to mRNA length, suggesting that the contact between the SREs in the 3′ UTR and the 5′ end of the RNA might be established in a manner that differs from the contact between the poly(A) tail and the cap.

Keywords: 5′–3′ interaction; closed-loop; mRNA decay; poly(A) tail; translational repression

INTRODUCTION

Eukaryotic mRNAs are linear polymers. They invariably have a 7-methyl guanosine cap structure at their 5′ end, which is followed by a typically short 5′ UTR, the open reading frame, a 3′-UTR of highly variable length, and, with few exceptions, a poly(A) tail at the 3′ end. The linear form of mRNAs is used in translation in a correspondingly linear fashion: Translation preinitiation complexes containing the small ribosomal subunit assemble at the 5′ cap and then locate the initiation codon by scanning in a 3′ direction. At the initiation codon, the large ribosomal subunit joins the complex, and the assembled ribosome continues to move toward the 3′ end, translating the open reading frame until it reaches a stop codon. Surprisingly in view of the linear structure of mRNAs and their linear decoding by ribosomes, communication between the 5′ and 3′ ends is integral to mRNA function and its regulation. Such communication almost certainly involves direct or indirect physical interaction; a specific form in which the mRNA ends are thought to interact has been dubbed the "closed-loop" model (Jacobson 1996; Thompson and Gilbert 2017; Vicens et al. 2018).

Three types of 5′–3′ interactions have been described: First, the 3′ poly(A) tail strongly stimulates the initiation of translation (Gallie 1991; Iizuka et al. 1994; Tarun and Sachs 1995; Wickens et al. 2000) through a protein-mediated association with the 5′ end: The cytoplasmic poly(A) binding protein (PABPC), which covers the poly(A) tails of cytoplasmic mRNAs, also associates with the translation initiation factor eIF4G, which in turn binds the cap-binding protein eIF4E. This chain of interactions forms the "closed-loop." As a result, the complex of cap-bound initiation factors is stabilized, and recruitment of the small ribosomal subunit at the 5′ end of the mRNA is facilitated (Tarun

[1]**Present address:** Institute of Molecular Systems Biology, ETH Zürich, HPT E 53, 8093 Zürich, Switzerland

Corresponding author: ewahle@biochemtech.uni-halle.de

Article is online at http://www.rnajournal.org/cgi/doi/10.1261/rna.073759.119.

© 2020 Kluge et al. This article is distributed exclusively by the RNA Society for the first 12 months after the full-issue publication date (see http://majournal.cshlp.org/site/misc/terms.xhtml). After 12 months, it is available under a Creative Commons License (Attribution-NonCommercial 4.0 International), as described at http://creativecommons.org/licenses/by-nc/4.0/.

and Sachs 1996; Imataka et al. 1998; Wells et al. 1998; Park et al. 2011). Poly(A) tail or PABPC can also promote translation initiation through additional mechanisms (Gray et al. 2000; Kahvejian et al. 2005). Interestingly, histone mRNAs and some viral RNAs lacking poly(A) tails and/or the cap have evolved alternative mechanisms of 5′–3′ interactions that favor translation (Piron et al. 1998; Kühn and Wahle 2004). A second 5′–3′ interaction occurs in mRNA decay: The initial step in mRNA decay is deadenylation, that is, the loss of the poly(A) tail by 3′ exonuclease activity. As first shown in *S. cerevisiae* and later confirmed in mammalian and *Drosophila* cells, deadenylation is a prerequisite for the second step, hydrolytic removal of the 5′ cap structure (Decker and Parker 1993; Couttet et al. 1997; Bönisch et al. 2007). Several mechanisms have been proposed. For example, eIF4E protects the cap against hydrolysis (Schwartz and Parker 2000). Thus, stabilization of eIF4E binding via eIF4G and PABPC may contribute to inhibition of cap hydrolysis by the poly(A) tail, that is, to some extent the dependence of cap hydrolysis on deadenylation may be just another functional consequence of the same 5′–3′ interaction that is important in translation (but see Coller et al. 1998). As an alternative or additional set of interactions linking deadenylation with cap hydrolysis, the 3′ ends of deadenylated mRNAs are decorated with the Lsm1-7 complex. The Lsm complex associates with Pat1, which in turn binds the decapping enzyme Dcp2; as a consequence, recruitment of the decapping enzyme is favored by mRNA deadenylation (Ling et al. 2011; Sharif and Conti 2013; Charenton et al. 2017). A third type of 5′–3′ interaction in mRNA is the repression of translation by RNA binding proteins or miRNAs associating with specific sites in the 3′-UTR. Both types of regulators can inhibit translation indirectly, by accelerating loss of the poly(A) tail. However, a direct inhibition of translation initiation occurs either as an additional or, in the case of some RNA binding proteins, the only mechanism. In many of the better understood cases, 3′-UTR-bound regulators interfere with initiation by blocking events at the 5′ cap structure, that is, at the very beginning of the translation cycle (Colegrove-Otero et al. 2005; Jonas and Izaurralde 2015).

All three types of 5′–3′ interactions entail two related problems: First, the two ends have to meet. This is not trivial in view of the great length of some mRNAs. Second, the interactions only make biological sense if they occur in *cis*, that is, if the poly(A) tail or regulatory molecule bound to the 3′-UTR affects events at the 5′ end of its own mRNA as opposed to the large excess of other 5′ ends present in the cell. It is unknown how 5′–3′ interactions are established in *cis*. We can envision the following possibilities: In the first, the two ends meet by three-dimensional diffusion (i.e., "through solution") (Fig. 1A). Because the two ends are tethered to each other by the mRNA body, one can imagine that the effective concentration of the *cis* 5′ end in the vicinity of the 3′ end (or regulatory site in the 3′-UTR) is sufficiently high to permit an association and to outcompete *trans* 5′ ends. A second, fundamentally different mechanism would be the establishment of a 5′–3′ interaction along the RNA backbone. One could imagine, for example, that a processive helicase, bound to the 3′-UTR as part of a regulatory complex, threads the mRNA through itself until it reaches the 5′ end (Fig. 1B). A protein complex polymerizing along the RNA would serve the same purpose (Fig. 1C; Jeske et al. 2011; Götze et al. 2017). Such mechanisms would eliminate any concentration dependence and establish a *cis* interaction in a fool-proof manner. Finally, an intermediate mechanism seems possible, in which several copies of a regulatory protein bound, directly or indirectly, to the 3′-UTR can grab additional internal segments of the mRNA and incorporate them into the RNP (Fig. 1D).

In our attempts to experimentally test aspects of these speculations, we have made use of an in vitro system

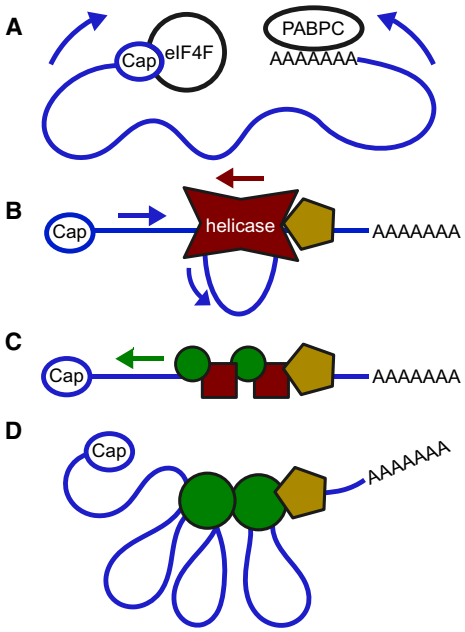

FIGURE 1. Four hypothetical ways to establish end-to-end interactions in an mRNA molecule. (*A*) Interaction "through solution": The two ends are tethered to each other through the mRNA body, but otherwise move independently in solution. EIF4F is the complex containing the cap-binding protein eIF4E and the PABPC-interacting protein eIF4G. (*B*) Interaction by threading: A protein complex stably associated with the 3′-UTR contains a helicase that threads the RNA through itself until the 5′ end is reached. Arrows indicate the direction of RNA threading (blue) and helicase movement (brown). (*C*) Interaction by polymerization: A protein complex stably associated with the 3′-UTR nucleates the assembly of a protein coat along the mRNA. The arrow indicates the direction of polymerization. (*D*) Interaction by noncontinuous binding: A protein complex primarily associated with the 3′-UTR can grab neighboring segments of the same RNA without moving strictly along the backbone. Incorporation of additional subunits into the protein complex permits the engagement of additional RNA segments.

that reproduces key aspects of the translational regulation of the *Drosophila nanos (nos)* mRNA (Jeske et al. 2006, 2011; Götze et al. 2017). In *Drosophila* eggs, a small fraction of the *nos* RNA is localized in the pole plasm at the posterior pole, whereas the larger fraction is uniformly distributed throughout the egg (Wang and Lehmann 1991; Bergsten and Gavis 1999). Exclusive translation of the localized *nos* RNA fraction (Ephrussi and Lehmann 1992; Smith et al. 1992; Gavis and Lehmann 1994; Zaessinger et al. 2006) is essential for the formation of the anterior–posterior axis of the embryo (Wang and Lehmann 1991; Gavis and Lehmann 1992). Translation of the nonlocalized fraction is repressed, and the RNA is degraded during the first 2–3 h of embryonic development (Gavis and Lehmann 1994; Dahanukar and Wharton 1996; Bashirullah et al. 1999). Among the sequences inhibiting translation of nonlocalized *nos* RNA are two Smaug recognition elements (SREs), which serve as binding sites for the repressor protein Smaug (Dahanukar and Wharton 1996; Smibert et al. 1996, 1999; Dahanukar et al. 1999). Smaug induces deadenylation as the first step in the degradation of *nos* RNA (Semotok et al. 2005; Zaessinger et al. 2006), and this is reproduced in an extract of *Drosophila* embryos of the appropriate stage (Jeske et al. 2006). In the same extracts, translation of reporter RNAs containing two SREs in their 3′-UTRs is strongly repressed at the initiation step, independently of deadenylation. A point mutation in both SREs prevents both deadenylation and repression (Jeske et al. 2006). Importantly in the context of the present paper, translation of unregulated reporter RNAs in the embryo extract is significantly stimulated by a 5′ cap and a 3′ poly(A) tail (Jeske et al. 2006, 2011). Thus, two types of 5′–3′ interactions—repression of translation initiation from the 3′-UTR and stimulation of translation initiation by the poly(A) tail—can be examined in the same experimental system.

SRE-dependent translational repression is effected by a protein complex that contains, in addition to Smaug, the proteins Cup, Me31B, Trailer hitch, Belle, PABPC, and eIF4E (Jeske et al. 2011; Götze et al. 2017). Complex formation is slow and sensitive to ATP depletion; once formed, the repressor complex is kinetically very stable (Jeske et al. 2011). Within the complex, Cup associates with Smaug and also binds eIF4E, thereby displacing eIF4G. This variation of the closed-loop structure contributes to the inhibition of translation (Nelson et al. 2004; Jeske et al. 2011). However, experimental observations indicate that the SRE-dependent complex also inhibits translation by an additional mechanism (Jeske et al. 2011). As the repressor complex appears to be ATP-dependent and contains two DEAD-box proteins, Me31B and Belle, one might envision that tracking of the RNA backbone is involved in the establishment of a contact between the 3′-UTR-bound repressor complex and the mRNA 5′ end to inhibit translation initiation. An alternative suggestion is based on the observation that the complex contains multiple copies of Me31B and its partner Tral, in proportion to the total length of the SRE-containing RNA. Thus, these two interacting proteins may form a protective "coat" on the RNA, preventing ribosome access. Such a mechanism would also guarantee that translation inhibition occurs in *cis* (Götze et al. 2017).

Here we have generated chimeric mRNA constructs in which an RNA fragment containing a 5′ cap and a reporter ORF was connected to a second, regulatory fragment through a protein bridge. The regulatory fragment carried two SREs and a poly(A) tail. In one version of these constructs, the 5′–3′ polarity of the regulatory fragment was also inverted with respect to the ORF fragment. Even though there was no continuous RNA backbone connecting the regulatory sites and the poly(A) tail with the 5′ end, poly(A)-dependent stimulation of translation initiation was efficient, suggesting that the poly(A) tail contacts the mRNA 5′ end through solution. This interpretation was supported by the observation that lengthening of the RNA substantially weakened the poly(A) effect, both in chimeric and in regular, nonchimeric RNAs. SRE-dependent inhibition of translation was also insensitive to disruption of the RNA backbone; thus, tracking of the RNA backbone plays no role in repression. However, in contrast to poly(A)-dependent stimulation of translation, SRE-dependent inhibition was largely insensitive to RNA length, suggesting that the SRE-bound repressor complex might contact the 5′ end by a different route compared to the poly(A) tail.

RESULTS

Construction of chimeric mRNAs

The hypothesis that 5′–3′ interactions might be established through solution (Fig. 1A) predicts that the manner in which the two ends are tethered to each other should be irrelevant for the interaction and its functional consequences. An example is provided by experiments in which polyadenylation of an RNA was promoted by the polyadenylation signal AAUAAA contributed by a second RNA molecule that was attached to the first via base-pairing, that is, in *trans* and in an inverted 5′–3′ orientation (Bienroth et al. 1991; Sheets et al. 1995). Accordingly, we designed chimeric RNAs composed of two molecules: The first was a capped nanoluciferase (nLuc) translation reporter, the second carried a poly(A) sequence with or without SREs. The second type of RNA will be referred to as "regulatory" independently of the absence or presence of SREs and their functionality (wild-type versus mutant control). The two RNA molecules were stably connected with each other by a biotin-streptavidin-biotin bridge as shown schematically in Figures 2A and 3A. If a 5′-3′ interaction can still function in such chimeras, a movement or

polymerization of proteins along the entire RNA backbone is unlikely to be essential for the establishment of the interaction.

In more detail, building blocks for chimeric RNAs were as follows (Figs. 2A, 3A): The translation reporter (nLuc RNA; 536 nt) had an m7GpppG cap at its 5′ end and contained the nLuc open reading frame (ORF) followed by a 30 nt 3′-UTR of irrelevant sequence. The RNA was derivatized at its 3′ end with a single biotin by ligation to biotin-pCp. Luciferase yields obtained from the nLuc RNA upon translation in either reticulocyte lysate or *Drosophila* embryo extract were not affected by biotinylation in the presence or absence of streptavidin (data not shown). All versions of the regulatory RNA contained a template-encoded poly(A) stretch of 60 nt, which was followed by 40 nt of mixed sequence. In regular, uninterrupted mRNAs, such an internal poly(A) "tail" functions normally in the stimulation of translation but is protected from SRE-dependent degradation (Jeske et al. 2011). One version of the regulatory RNA (140 nt) contained only this internal poly(A) tail but no SRE. A second version (305 nt) contained, in addition, the "translation control element" (TCE) of the *Drosophila nos* mRNA (Dahanukar and Wharton 1996), which harbors two SREs. A control RNA (SRE$^-$) had a single point mutation in each SRE. These mutations completely abolish SRE function, but do not affect a minor extent of translation repression dependent on the Glorund binding site (Jeske et al. 2006; Kalifa et al. 2006; Tamayo et al. 2017). All regulatory RNAs were biotinylated by either of two different methods: In the first, priming of transcription with a biotin-ApG primer introduced a single biotin at the 5′ end. When this regulatory RNA was appended to the nLuc RNA via a streptavidin bridge, the normal 5′–3′ polarity was maintained throughout the construct ("forward" constructs; Fig. 3A). In a more radical approach, the regulatory RNA was synthesized with an ApppG cap, and a single biotin was appended to the 3′ end by ligation to biotin-pCp. Fusion of this regulatory RNA to the nLuc RNA via streptavidin not only interrupted the RNA backbone, but also inverted the 5′–3′ polarity of the regulatory RNA in relationship to the nLuc RNA ("flipped" constructs; Fig. 3A). Incubation of any of the biotinylated RNAs with streptavidin followed by native gel electrophoresis resulted in one and sometimes two retarded bands, presumably reflecting the binding of one or two RNAs to one streptavidin molecule (Fig. 2B; compare lanes 1–3 and 4–6). The absence of nonbound regulatory RNA showed that the efficiency of 5′ biotinylation

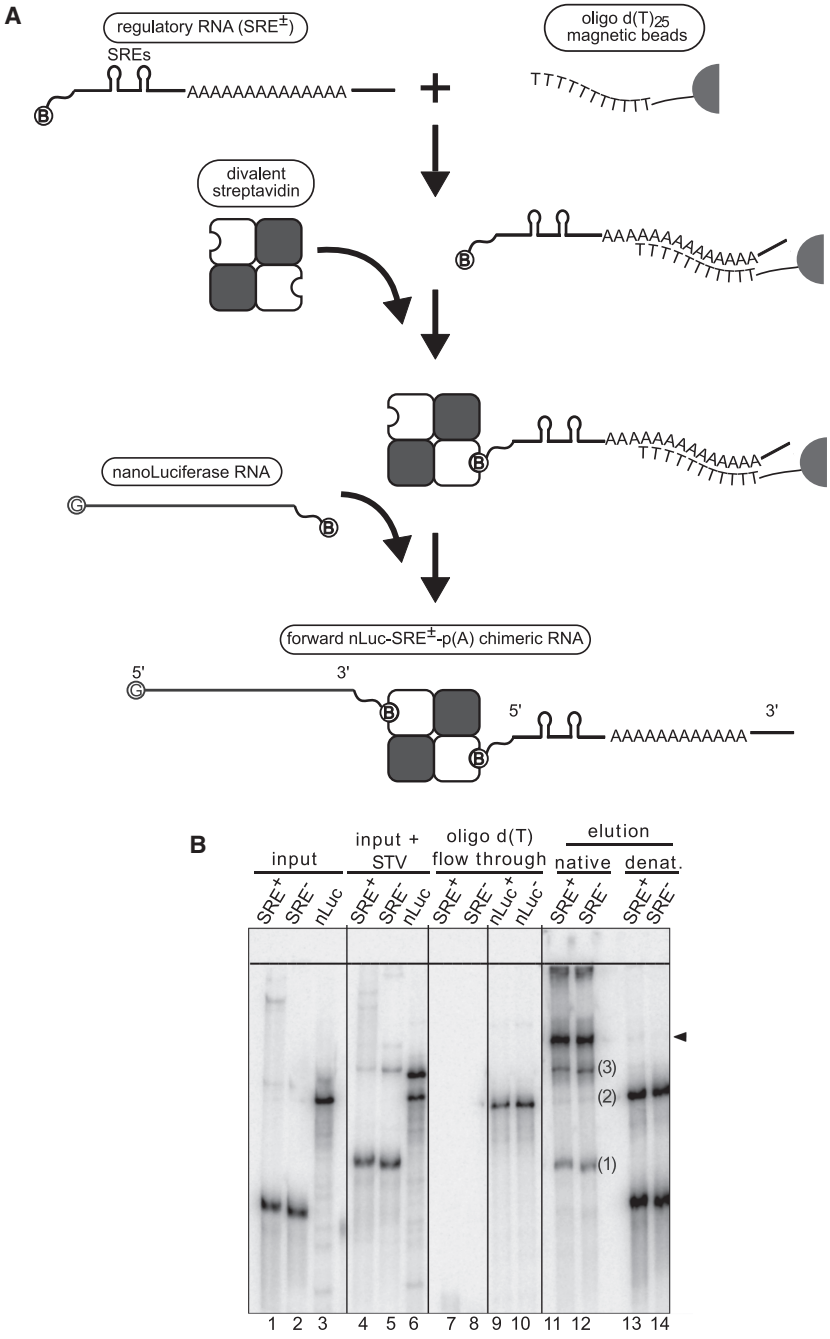

FIGURE 2. (Legend on next page)

approached 100%, whereas remaining nonbound nLuc RNA suggested that efficiencies of 3′ biotinylation were 50%–70%.

Wild-type streptavidin is a homotetramer and thus provides four biotin binding sites. This would complicate the preparation of defined pairs of one nLuc RNA and one regulatory RNA. Therefore, divalent streptavidin, prepared as previously described (Howarth et al. 2006; Materials and Methods), was used for all experiments.

The steps leading to the assembly of chimeric RNAs (Fig. 2A) were routinely controlled by native gel electrophoresis (Fig. 2B). Regulatory RNAs were first bound to oligo(dT) beads through the internal poly(A) tracts of the RNAs; the absence of RNA in the flow-through demonstrated complete binding (Fig. 2B, lanes 7,8). The beads were then incubated with excess divalent streptavidin and subsequently with the nLuc RNA. Unbound nLuc RNA was removed by washing (Fig. 2B, lanes 9,10) and chimeric RNA eluted with low-salt buffer. A prominent new band in the eluted fraction was indicative of the desired construct (Fig. 2B, lanes 11,12). Denaturation restored the two starting RNAs, providing clear evidence of the hybrid nature of the eluted RNAs (Fig. 2B, lanes 13,14).

Comparison to the starting material revealed that the preparations of chimeric RNA still contained some regulatory fragments not fused to nLuc RNA (bands labeled 1 and 3 in Fig. 2B, lanes 11 and 12). These were less abundant than the chimeric RNA (<40% of the total regulatory RNA present in the eluate) and were not expected to affect translation as they contained no open reading frame and, at the sub-nanomolar concentrations present during translation assays, would not act as competitors for Smaug binding (Jeske et al. 2011). The preparation also contained some nLuc RNA not fused to a regulatory fragment (band labeled 2 in Fig. 2B, lanes 11 and 12; 10%–20% for the forward and 10%–35% for the flipped constructs of the total nLuc RNA present in the eluate). Results of the translation assays (see below) suggested that these RNAs had no significant effects either. Note that the amounts of nonfused RNAs are upper estimates assuming complete stability of the RNA-streptavidin complexes in formamide-containing gel loading buffer in the absence of boiling.

Altogether the data demonstrate an efficient preparation of intact hybrid RNAs composed of a constant 5′ half with the nLuc reporter ORF separated by a biotin-streptavidin bridge from regulatory RNAs containing poly(A) with or without SREs.

Both poly(A)-dependent stimulation and SRE-dependent repression of translation function with chimeric mRNAs

The various chimeric RNAs used for translation experiments are displayed in Figure 3A. For comparison, we used a 3′ biotinylated nLuc RNA lacking any regulatory fragment, that is, containing no poly(A): As assembly of the chimeric RNAs depended on the poly(A) stretch, no poly(A)$^-$ chimeric RNA could be constructed, and the extent of poly(A) stimulation had to be measured by comparison to nonchimeric, "bare" nLuc RNA.

All RNAs were preincubated at 0.2 nM in reaction mixtures with *Drosophila* embryo extract under conditions that promote assembly of the SRE-dependent repressor complex but do not permit translation. Translation was then started by the addition of an ATP-regenerating system (Jeske et al. 2011), and luciferase activity was measured 30 min later. Figure 3B,C shows luciferase yields in representative experiments. To check to which extent observed differences in translation yields were caused by variations in RNA quality, all RNA preparations were controlled by translation in RRL, which is not affected by SREs (Jeske et al. 2006) and weakly or not at all by poly(A) (Fig. 3D,E; Gallie 1991). Thus, different luciferase yields of the chimeric RNAs in RRL reflected batch-dependent differences in RNA quality, and translation yields in embryo extract were corrected according to yields in RRL. The resulting

FIGURE 2. Assembly of chimeric RNA constructs. (*A*) Outline of the procedure. Regulatory RNAs contained a 5′ biotin, two SREs (SRE$^+$ = WT or SRE$^-$, that is, with an inactivating point mutation in each SRE) and a poly(A) sequence, which was protected against deadenylation by an N_{40} sequence at the 3′ end. Alternatively, regulatory RNA was used that carried a poly(A) sequence but no SREs (not shown). The regulatory RNA was hybridized to immobilized oligo(dT), then divalent streptavidin and the capped and 3′-biotinylated nLuc reporter RNA were added in a stepwise manner. The chimeric construct was eluted in low-salt buffer. The scheme shows the assembly of forward constructs. Flipped constructs were assembled in the same manner, but 3′-biotinylated regulatory RNAs were used. For a full description of the procedure, see Materials and Methods. (*B*) Assembly of chimeric RNAs assayed by native gel electrophoresis. Chimeras [forward-SRE$^\pm$p(A)] were assembled as described in panel *A* and Materials and Methods. The figure shows the analysis of input and product RNAs by electrophoresis through a 5% nondenaturing polyacrylamide gel. Lanes *1–3* display the input RNAs as indicated. Lanes *4–6* demonstrate the retardation of input RNAs upon mixing with divalent streptavidin (STV). Two retarded bands in one lane are presumably due to binding of one or two RNAs to one molecule of streptavidin. Lanes *7*, *8* show the flow-through of the oligo (dT) matrix after loading with regulatory RNAs; binding was essentially complete. Lanes *9* and *10* show the flow-through of excess nLuc RNA in the last assembly step. "nLuc$^+$"′ and "nLuc$^-$" refer to the nLuc RNAs from the assembly reactions with SRE$^+$ and SRE$^-$ regulatory RNAs, respectively. Lanes *11* and *12* show the eluate in formamide-containing loading buffer without heat denaturation. The main band (arrowhead) is a novel species that we interpret as the desired chimeric RNA. Upon heat denaturation (lanes *13*, *14*), the input RNAs are restored. Residual amounts of input RNAs can be detected: Based on a comparison to other lanes in this gel, numbered bands are (1) a complex between one regulatory RNA and streptavidin, (2) bare nLuc RNA, and (3) a complex between two regulatory RNAs and streptavidin. The broken line indicates the upper end of the gel.

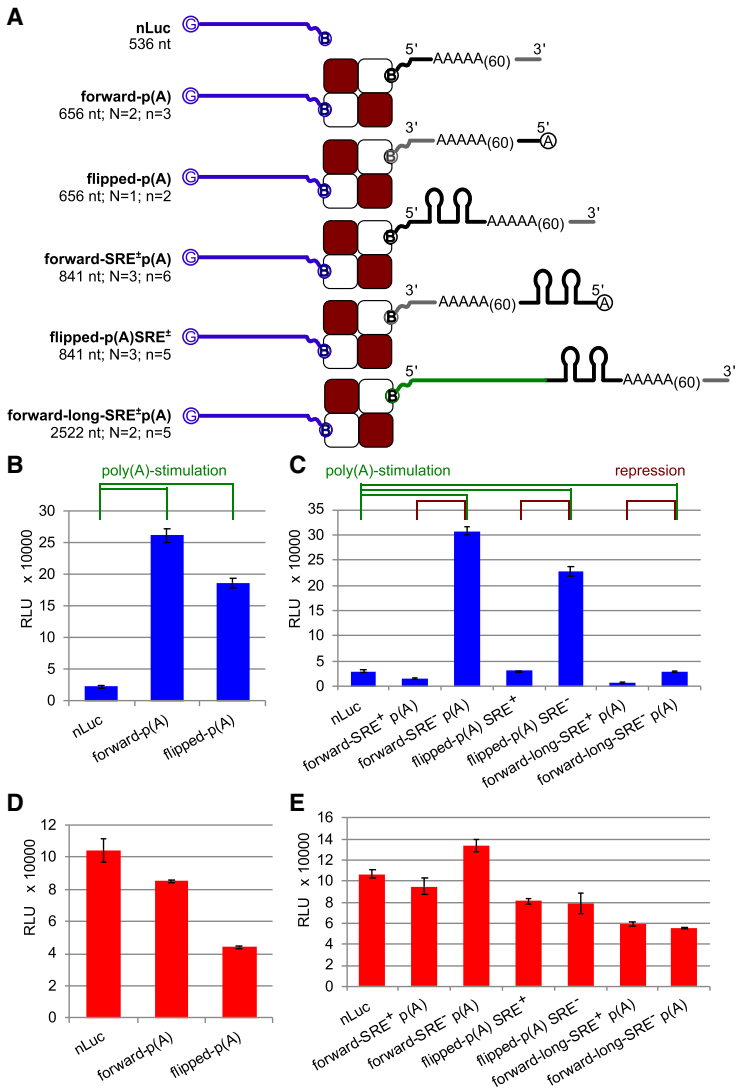

FIGURE 3. Translation of chimeric RNAs is stimulated by poly(A) tails and repressed by SREs. (*A*) Scheme of chimeric constructs. All nLuc RNAs (blue) had a 5′ m7G cap and a 3′ biotin. Regulatory RNAs had either a 5′ biotin combined with an unmodified 3′ end (forward constructs) or a 5′ A cap combined with a 3′ biotin (flipped constructs). The green RNA section in the forward-long-SRE$^{\pm}$p(A) construct represents the firefly luciferase stuffer fragment (see text). Regulatory RNAs attached to the *right* of the central divalent streptavidin were as described in Figure 2 and the text. All SRE-containing RNAs were synthesized as SRE^{+} and SRE^{-} variants as indicated. "N" indicates the number of independent chimeric RNA preparations tested in translation. The number of independent translation experiments (each carried out as three technical replicates) is represented by "n." Each type of RNA was tested in at least three batches of embryo extract except the flipped-p(A) construct, which was tested in two batches. (*B*) Translation assays of nLuc and chimeric RNAs containing poly(A) segments in forward and flipped orientations. RNAs were assayed in parallel for translation in *Drosophila* embryo extract as described in Materials and Methods. The pairwise comparisons used to calculate poly(A)-dependent stimulation are indicated at the *top*. (*C*) Assays as in *B* were carried out with the chimeric constructs containing poly(A) segments plus SREs. The pairwise comparisons used to calculate poly(A)-dependent stimulation or SRE-dependent repression, respectively, are indicated at the *top*. (*D*,*E*) The same RNA preparations as in *B* and *C* were translated in parallel in rabbit reticulocyte lysate (RRL). It was assumed that differences in luciferase activities represented variable qualities of the RNA preparations rather than SRE- or poly(A)-effects. Numbers from such assays were therefore used to correct luciferase yields obtained in embryo extract in Figures 4, 7, and 8. Panels *B* through *E* show the results of single representative experiments with error bars representing the standard deviations of three technical replicates.

correction factors were small compared to the poly(A)- and SRE-dependent effects observed in embryo extract (Figs. 3, 4), that is, the qualities of RNA preparations were reasonably consistent. Consequently, the results described below were also reproducible with independent RNA preparations (Fig. 3A).

Data from multiple experiments are summarized in Figure 4. Both corrected and uncorrected results are presented to demonstrate that correction on the basis of RRL translation did not affect our conclusions. The extent of poly(A)-dependent stimulation of translation was determined from a comparison of the bare nLuc RNA to several types of chimeric RNA constructs carrying poly(A) in their regulatory fragments as indicated in Figure 3B,C. The results consistently revealed a strong stimulation that was independent of the relative 5′–3′ orientations of the fused RNA segments: Regulatory fragments containing only poly(A) but no SREs effected an 11- to 15-fold stimulation in forward and flipped orientation, respectively (Figs. 3B, 4A). Similar data were obtained when the regulatory fragments combined a poly(A) sequence with a nonfunctional SRE (SRE^{-}): In numerous experiments, the average stimulation factors for the forward and flipped constructs, respectively, were 8.4 and 7.5 (Figs. 3C, 4A). The corresponding SRE^{+} constructs were not considered for the poly(A) effect, as their comparison to nLuc RNA would have involved an uninterpretable mixture of repression and stimulation. The forward-long-SRE$^{\pm}$p(A) constructs will be discussed below.

A comparison of equivalent chimeras containing either SRE^{+} or SRE^{-} regulatory fragments revealed a strong SRE-dependent repression of translation. On average, repression was 94.5% in the forward and 82% in the flipped orientation (Figs. 3C, 4B), that is, residual translation of the SRE^{+} constructs was 5.5% and 18%, respectively, of the corresponding SRE^{-} constructs. Thus, both poly(A)-

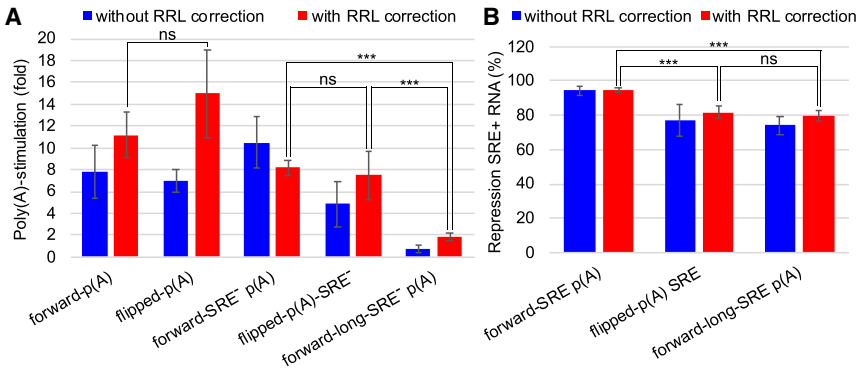

FIGURE 4. Summary of the results of translation assays with chimeric RNAs. (*A*) Poly(A)-dependent stimulation. Stimulation factors were calculated from pairwise comparisons to the bare nLuc RNA as indicated in Figure 3B,C ($P = 0.04$ for forward-long-SRE$^-$ RNA and $P \leq 1.6 \times 10^{-4}$ for all others). SRE$^+$ RNAs were not considered, as explained in the text. (*B*) SRE-dependent repression. Numbers were calculated from pairwise comparisons of SRE$^+$ and SRE$^-$ variants as shown in Figure 3C ($P \leq 1.3 \times 10^{-4}$ for all RNAs). All data in *A* and *B* are presented both corrected for translation efficiency in RRL (red bars) and without correction (blue bars). Correction factors in individual experiments were at most 2 and typically lower. Error bars indicate the standard deviation based on the numbers of independent experiments reported in Figure 3A. The statistical significance of the pairwise comparisons indicated by brackets is indicated by (***) ($P < 0.001$) and ns (nonsignificant).

dependent stimulation and SRE-dependent repression of translation initiation were functional with the chimeric constructs, independently of the orientation of the regulatory sequences.

Results were reproducible with independent batches of embryo extract, although the magnitude of the effects was batch-dependent, as reflected in the relatively large error bars in Figure 4 and also in Figures 7 and 8 (see below). Both with respect to poly(A)-dependent stimulation and SRE-dependent repression, the conclusions drawn from the single time-point experiments were supported by translation kinetics (Supplemental Fig. 1). The magnitudes of stimulation by poly(A) and repression by SREs observed for the chimeric RNAs were similar to what had previously been reported for continuous mRNAs (Jeske et al. 2006, 2011). The strong effects show that contamination of the chimeric RNAs by bare nLuc RNA had no significant effect on the results: As luciferase yields from the bare nLuc RNA are poor in embryo extract, contamination by this RNA is expected to make a quantitatively significant contribution only in the case of the SRE$^+$ constructs, which are also poorly translated; thus, the extent of SRE-dependent repression might be somewhat underestimated. This would not affect our conclusions.

Stimulation by poly(A) and inhibition by the SREs were not due to stability effects: Recoveries of the reference RNA, biotinylated nLuc RNA, at the end of incubation in three different batches of embryo extract were between 66% and 88%, slightly higher than the recoveries of chimeric RNAs (see below). Thus, low luciferase yields from the nLuc RNA were not a consequence of instability, that is, the stimulatory effect of poly(A) was not due to RNA stabilization. Stabilities of the chimeric constructs were tested by adsorption to oligo(dT) beads at the beginning and the end of the incubation, followed by RNA purification under conditions that inactivate streptavidin and analysis by denaturing gel electrophoresis. Recovery of both the regulatory RNA and the nLuc RNA confirmed stability of the streptavidin bridge under experimental conditions (Fig. 5). In agreement with earlier observations (Jeske et al. 2006, 2011; Götze et al. 2017), slightly higher stability of the SRE$^+$ RNA constructs ruled out SRE-dependent mRNA decay as an explanation for lower luciferase yields.

Poly(A)-dependent stimulation and SRE-dependent inhibition of

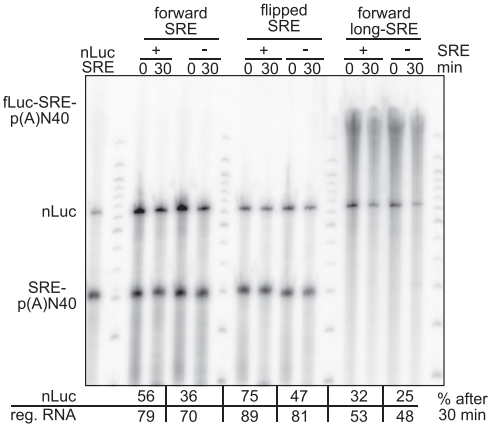

FIGURE 5. Recoveries of chimeric RNAs after incubation in *Drosophila* embryo extract. Forward or flipped constructs containing the SRE$^+$ or SRE$^-$ regulatory RNAs depicted in Figure 3 were incubated in embryo extract for 30 min at 25°C. One sample was oligo(dT)-purified immediately (0 min), a second sample at the end of the incubation. RNAs were analyzed by denaturing gel electrophoresis (see Materials and Methods). The first lane contains a mixture of nLuc and a regulatory RNA as markers. Recoveries of the nLuc and regulatory RNAs are given at the *bottom*. RNA recovered at the 0 min time point was set to 100%. As recovery on oligo(dT) beads was based on the poly(A) stretch in the regulatory RNA, copurification of the nLuc RNA demonstrated the stability of chimeras. Furthermore, SRE$^+$-containing constructs were more stable than SRE$^-$ constructs; thus, the lower translation yield of SRE$^+$ RNAs was not due to RNA destabilization. Recoveries of regulatory RNAs were generally higher, presumably due to their small size (compare the small regulatory RNAs in the first two sets to the long fLuc-containing regulatory RNA in the third set). Recall that not all regulatory RNAs were bound to nLuc RNA (compare Fig. 2B).

translation of the chimeric RNAs demonstrates that 5′–3′ interactions in these RNAs can be established independently of a continuous RNA backbone.

An authentic SRE-dependent repressor complex assembles on chimeric RNA constructs

The repressed chimeric RNAs shared several previously described characteristics of uninterrupted repressed RNAs: First, SRE-dependent repression of the chimeras was amplified by a preincubation before the start of translation (Jeske et al. 2011) (data not shown). Second, formation of the repressor complex on chimeric RNAs caused them to sediment more rapidly in sucrose gradient centrifugation than their nonrepressed counterparts, as observed for non chimeric RNAs (Fig. 6A; Götze et al. 2017). Third, both RNA components of the repressed chimeras were relatively resistant against RNase degradation compared to their nonrepressed counterparts (Fig. 6B; Götze et al. 2017). SRE-dependent stabilization was more pronounced for the regulatory RNA than for the nLuc RNA, but stabilization of the nLuc RNA was seen in both flipped and forward constructs. The nLuc RNA was also stabilized against endogenous RNases of the embryo extract by fusion with an SRE$^+$ regulatory RNA (Fig. 5), as pointed out above. If one assumes that rapid sedimentation and resistance to RNase attack reflect the formation of a protein complex sequestering the RNA from translation (Götze et al. 2017), the results indicate that SRE-dependent formation of this complex can circumvent the streptavidin roadblock and extend into the nLuc RNA.

Poly(A)-dependent stimulation of translation is sensitive to RNA length, but SRE-dependent repression is not

The simplest interpretation of the results presented so far is that sequences in the regulatory RNA fragments contact the 5′ ends of the nLuc reporter RNAs through solution (Fig. 1A). Such end-to-end interactions should be less efficient for longer molecules (see Discussion). In order to test this prediction, we first

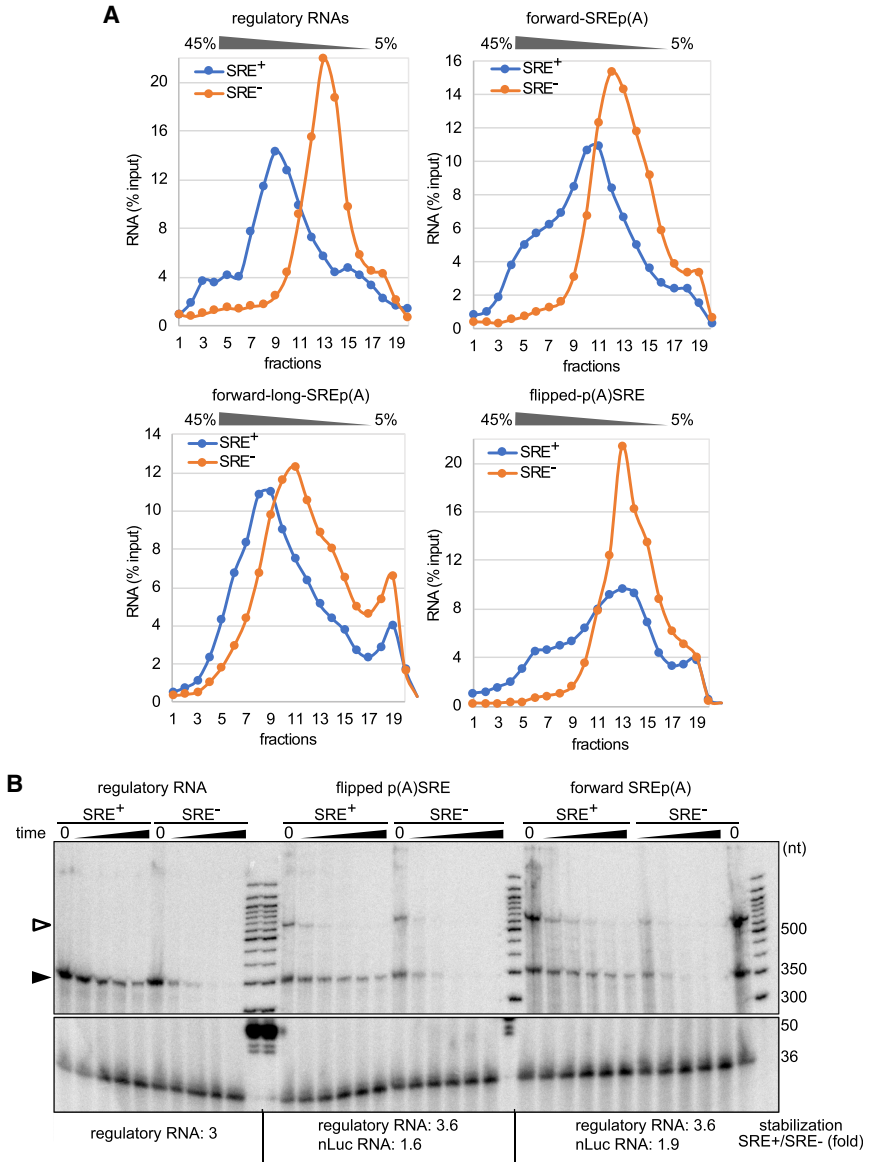

FIGURE 6. Analysis of the SRE-dependent repressor complex assembled on chimeric RNAs. (*A*) Rapid sedimentation of repressed RNAs. Radiolabeled chimeric RNAs were incubated for 30 min in *Drosophila* embryo extract under preincubation conditions. Radiolabeled regulatory RNAs not fused to the nLuc reporter (*top left*) were used as positive controls. At the end of the incubation, 200 µL aliquots were analyzed by sucrose gradient centrifugation as previously described (Götze et al. 2017). Radioactivity in each fraction was measured by scintillation counting. Formation of the repressor complex resulted in accelerated sedimentation, as reported before (Götze et al. 2017). (*B*) Partial RNase resistance of repressed RNAs. Regulatory RNA by itself as well as flipped and forward chimeric constructs, all in the SRE$^+$ and SRE$^-$ versions, were incubated in *Drosophila* embryo extract under preincubation conditions, then a time-course of RNase digestion was performed as described in Materials and Methods. Time points were taken at 5 min intervals. A radiolabeled synthetic RNA oligonucleotide was added before RNA purification and served as a recovery control (*bottom* part of the gel). White and black arrowheads indicate the nLuc and the regulatory RNA, respectively. Stabilization factors were calculated by comparison of the SRE$^+$ RNA and SRE$^-$ RNA half-lives and are listed at the *bottom*.

generated an additional pair of SRE$^+$ and SRE$^-$ chimeric RNAs in which the firefly luciferase ORF as a stuffer fragment was attached to the 5′ end of the regulatory RNA, extending the total construct to a length of 2522 nt [forward-long-SRE$^\pm$p(A) constructs; Fig. 3A]. In these constructs, the firefly luciferase ORF is not expected to be translated due to its downstream position in the chimera and the lack of a cap structure. The absence of firefly luciferase activity was confirmed experimentally (data not shown). As predicted from less efficient end-to-end interaction in longer polymers, translation of the nonrepressed, SRE$^-$ version of this RNA was less than twofold higher than that of the reference nLuc RNA (Figs. 3, 4). Thus, poly(A)-dependent stimulation of translation was no longer very effective. Although the extended regulatory RNA fragment was less stable than the shorter ones (Fig. 5), the slight decrease in stability was unable to quantitatively explain the almost complete absence of poly(A) stimulation. Unexpectedly, SRE-dependent repression of translation proved largely resistant against extension of the RNA (Figs. 3, 4). This also confirms that reduced stability of the regulatory fragment is not an issue in the interpretation of the results.

The expectation that end-to-end interactions are length-sensitive is not limited to chimeric RNAs. Therefore, we generated two additional series of regular, uninterrupted RNAs to determine how RNA length affects poly(A) stimulation and SRE-dependent repression. All RNAs contained the regulatory sequences close to their 3′ ends. In the first series (Fig. 7A), the 3′-UTR of the nLuc RNA was extended by the insertion of the maltose binding protein (MBP) coding sequence downstream from the nLuc stop codon. In the second series (Fig. 8A), the 3′-UTRs of RNAs containing the fLuc ORF were extended by either one or two copies of the MBP sequence inserted downstream from the fLuc stop codon. All RNAs were created as SRE$^+$ and SRE$^-$ versions. Importantly, these RNAs were also made with or without poly(A) tails (Figs. 7A, 8A), so that poly(A)-dependent stimulation could be assessed from the comparison of nearly identical RNAs and did not have to rely on a comparison to the short nLuc RNA. [Recall that poly(A)$^-$ versions of the chimeric constructs could not be made, as poly(A) was required for their assembly.] As above, poly(A)-dependent stimulation and SRE-dependent inhibition of translation were measured in *Drosophila* embryo extract, and RNA qualities were controlled by translation in RRL.

Each RNA was tested at 2 nM in all four combinations of SRE$^+$ and SRE$^-$, poly(A)$^+$ and poly(A)$^-$. As for the chimeric RNAs, poly(A)-dependent stimulation was assessed in the unrepressed (SRE$^-$) RNAs, that is, in the absence of the confounding effects of simultaneous repression. Conversely, the full extent of SRE-dependent repression is attained only with polyadenylated RNAs (Jeske et al. 2006, 2011). Therefore, SRE-dependent repression was assessed with poly(A)$^+$ RNAs. Figures 7 and 8 present the relevant pairwise comparisons, both with and without correction on the basis of RRL translation.

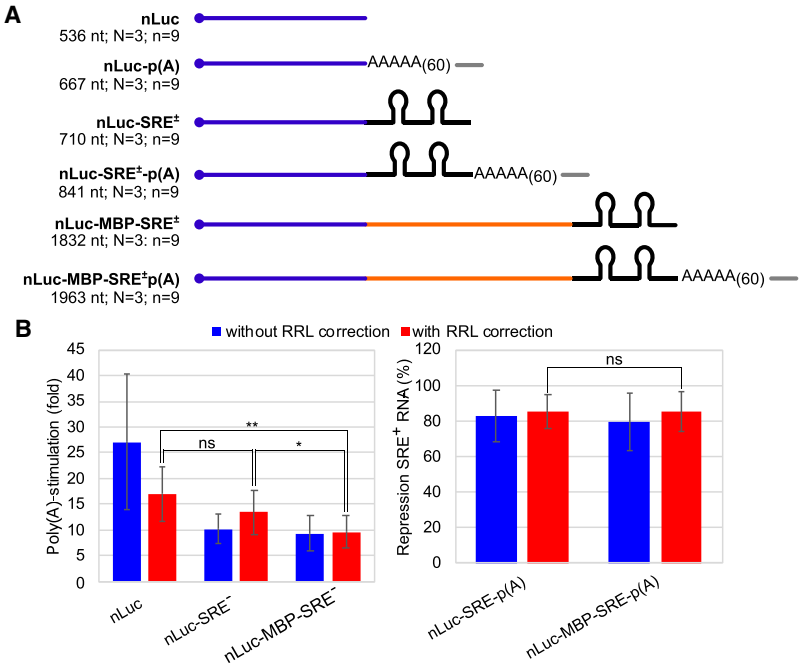

FIGURE 7. Length-dependence of poly(A)- and SRE-effects assayed in a series of RNAs based on nanoluciferase. (*A*) Scheme of the RNAs used. All contained an m7G cap and the nLuc ORF. They had poly(A) tails and/or SREs at their 3′ end as shown. All SRE-containing RNAs were synthesized in an SRE$^+$ and an SRE$^-$ version as indicated. The two RNAs at the *bottom* were extended by the ORF encoding MBP (orange line) inserted between the nLuc stop codon and the SREs. "N" indicates the number of independent RNA preparations assayed. Each of the three preparations of each RNA was tested in two to four independent batches of *Drosophila* embryo extract, resulting in nine independent experiments per RNA ("n"). (*B*) Summary of translation experiments carried out with the RNAs depicted *above*. Poly(A) stimulation, shown on the *left*, was calculated from the comparison of equivalent SRE$^-$ RNAs carrying a poly(A) stretch or not ($P \leq 3.8 \times 10^{-5}$). SRE-dependent repression, shown on the *right*, was calculated from the comparison of SRE$^+$ and SRE$^-$ RNAs that also carried a poly(A) tail ($P \leq 5.8 \times 10^{-4}$). Both stimulation and repression are shown with a correction for translational efficiency in RRL (red bars) and without correction (blue bars). Correction factors in individual experiments were typically between 1 and 1.5 and up to 3 in a few cases. Error bars indicate the standard deviation based on the numbers of independent experiments reported in *A*. The statistical significance of the pairwise comparisons indicated by brackets is indicated by (*) ($P < 0.05$), (**) ($P < 0.01$), and ns (nonsignificant).

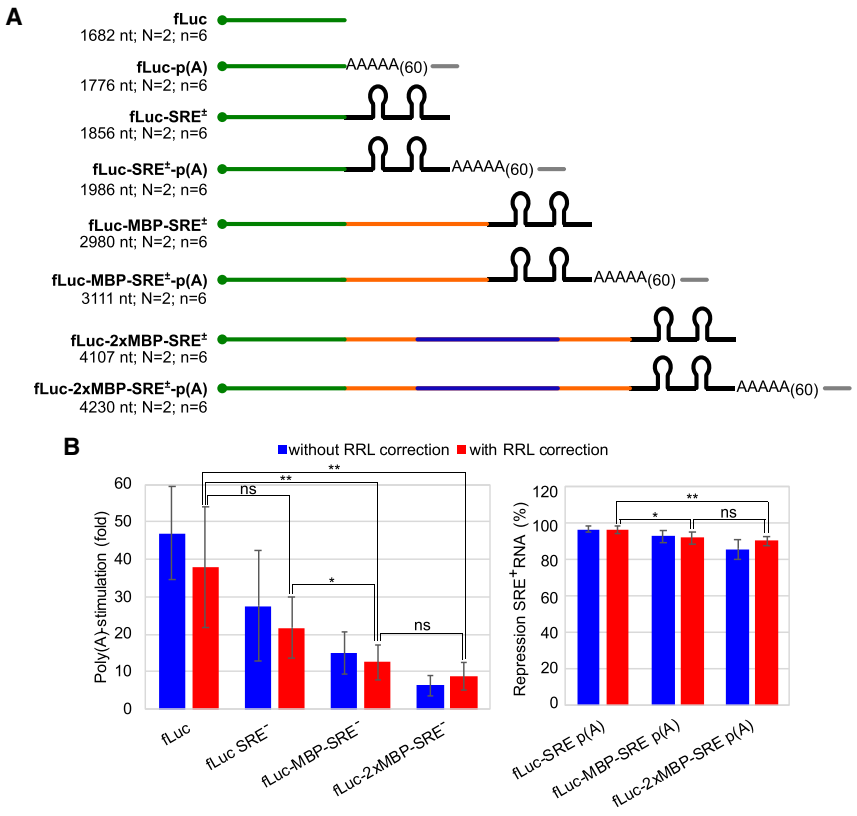

FIGURE 8. Length-dependence of poly(A)- and SRE-effects assayed in a series of RNAs based on firefly luciferase. (*A*) Scheme of the RNAs used: All contained an m7G cap and the fLuc ORF (green lines). They had poly(A) tails and/or SREs at their 3′ ends as shown. All SRE-containing RNAs were synthesized in an SRE^+ and an SRE^- version as indicated. The fLuc-MBP RNAs were extended by the ORF encoding MBP (orange lines) inserted between the fLuc stop codon and the SREs. For the fLuc-2xMBP RNAs, a second MPB ORF was inserted in the middle of the first MBP ORF (blue lines). "N" indicates the number of independent RNA preparations assayed. Each of the two preparations of each RNA was tested in three independent batches of *Drosophila* embryo extract, resulting in six independent experiments per RNA ("n"). (*B*) Summary of translation experiments carried out with the RNAs depicted *above*. Poly(A) stimulation, shown on the *left*, was calculated from the comparison of equivalent SRE^- RNAs carrying a poly(A) tail or not ($P \leq 1.3 \times 10^{-5}$). SRE-dependent repression, shown on the *right*, was calculated from the comparison of SRE^+ and SRE^- RNAs that also carried a poly(A) tail ($P \leq 1.1 \times 10^{-5}$). Both stimulation and repression are shown with a correction for translational efficiency in RRL (red bars) and without correction (blue bars). Correction factors were similar as in Figure 7. Error bars and indications of statistical significance of the comparisons indicated by brackets are as in Figure 7.

Within each series, lengthening of the RNA led to a significant drop in the stimulation of translation by poly(A). This is the result expected for an end-to-end interaction through solution (see Discussion). In striking contrast to poly(A)-dependent stimulation, SRE-dependent repression was almost completely insensitive to RNA length. This segregation of poly(A)-dependent stimulation from SRE-dependent repression of translation was observed in both series of nonchimeric RNAs and in the chimeric constructs.

Because of potential structure formation in 3′-UTRs, it is difficult to predict to which extent the end-to-end distance of the RNA is in fact increased by lengthening of the 3′-UTR. In contrast, coding sequences are straightened out by ribosome passage (see Discussion). Therefore, we mutagenized the stop codon in the fLuc-MBP-$SRE^{\pm}$ and fLuc-MBP-$SRE^{\pm}$-poly(A) constructs, generating translational fusions of fLuc with MPB. Limited tests of these RNAs (two independent batches of extract) showed that they behaved very similar to the parental RNA constructs: Stimulation of translation by poly(A) was 6.2-fold for the translational fusion and 6.6-fold for the parental construct tested in parallel. Repression by the SREs was 85% for the translational fusion and 75% for the parental construct tested in parallel. The results for the parental RNAs were similar to those in Figure 8. Thus, the effects of poly(A) tail and SREs are independent of the distribution of total sequence between ORF and 3′-UTR, at least in this set of constructs.

RNA stability was a particular concern in the experiments involving long RNAs: Since a longer RNA is a larger target for ribonucleases, weaker effects of the poly(A) tail or the SREs might be caused by a larger fraction of RNAs that have retained an intact ORF but lost their regulatory elements due to nuclease activity. However, two arguments suggest that this does not explain the results: First, since poly(A) tail and SREs were always in close neighborhood, nuclease activity should have led mostly to the simultaneous loss of both, that is, should have affected poly(A)- and SRE-dependent effects in a similar manner and would not explain the segregation observed. Second, direct assays suggested that stability differences were not responsible for the different translation yields observed: In three independent experiments, average recoveries of all nonchimeric RNAs after incubation in embryo extract were between ~65 and ~80%, that is, differences were small compared to differences in translation yields. No systematic effect of internal poly(A) stretches on RNA recoveries was observed. As noted above, SRE^+ RNAs were typically slightly more stable than SRE^- RNAs (data not shown).

Our interpretation of all experiments is based on the assumption that the effects of SRE and poly(A) tail reflect 5′–3′, that is, intramolecular interactions. However, poly

(A) is known to exert some stimulatory effects in *trans* (Munroe and Jacobson 1990). While the assumption of an intramolecular effect is more plausible due to the very low RNA concentrations used, we also tested whether either an SRE-containing short RNA or poly(A), added at 2 or 4 nM, would affect the translation of 2 nM fLuc RNA (Fig. 8) lacking either. No such effect was observed (data not shown). Therefore, the effects of SREs and poly(A) tail on translation observed with the *cis* constructs indeed reflect intramolecular 5′–3′ interactions.

In summary, an increase in mRNA length weakens stimulation of translation by a poly(A) tail. Together with the resistance of the poly(A) effect to a streptavidin linkage and to an inversion of 5′–3′ polarity in the mRNA, these results support an end-to-end interaction through solution. SRE-dependent repression of translation is also insensitive to a streptavidin roadblock. This makes any repression mechanism involving tracking of the RNA backbone unlikely. However, repression is largely insensitive to RNA length. This suggests the possibility that stimulation of translation by the poly(A) tail and repression of translation by the SRE-dependent repressor complex rely on different mechanisms to achieve an end-to-end interaction.

DISCUSSION

We have examined the mechanism by which regulatory elements close to the 3′ end of an mRNA establish contact with the 5′ end to affect the efficiency of translation. Stimulation of translation by the poly(A) tail was fully functional in chimeric RNAs in which the poly(A) tail was separated from the cap and the ORF by a protein bridge, even when this disruption of the RNA backbone was combined with an inversion of the 5′–3′ polarity of the poly(A)-containing 3′ RNA fragment in relationship to the ORF. The result is inconsistent with any mechanism of 5′–3′ communication that would involve tracking the RNA backbone from the 3′ end to the *cis* cap (Fig. 1B,C), but is consistent with an establishment of the 5′–3′ interaction through solution.

In principle, end-to-end interaction through solution should be sensitive to RNA length because the local concentration of one end of a linear polymer in the neighborhood of the other end decreases with increasing polymer length. For a structurally uniform polymer like DNA, this effect can be quantitatively predicted by mathematical modeling, and such predictions have been experimentally verified (Wang and Davidson 1966; Dugaiczyk et al. 1975). For RNA, lack of a uniform structure makes quantitative prediction more difficult. Computational and experimental investigations of "naked" long RNAs have led to the surprising conclusion that, due to secondary structure formation, the two ends are always close to each other, within a few nanometers, independently of the length of the RNA (Yoffe et al. 2011; Leija-Martínez et al. 2014; Lai et al. 2018). However, RNA conformation will be modified in vivo by protein binding, helicase activity (Guo and Bartel 2016) and, most importantly, ribosome transit (Lingelbach and Dobberstein 1988; Takyar et al. 2005), and the resulting removal of secondary structure will increase end-to-end distance (Lai et al. 2018). In agreement with this expectation, in situ imaging of translated mRNAs by simultaneous visualization of fluorescent probes hybridized to the two ends revealed relatively extended structures; treatments that induced ribosome release induced compaction (Adivarahan et al. 2018; Khong and Parker 2018). Thus, one can qualitatively predict that end-to-end interaction during translation should be sensitive to RNA length. In our experiments, poly(A)-dependent stimulation of translation did in fact become weaker with increasing RNA length. This is consistent with earlier data showing sensitivity of closed-loop formation to RNA length in yeast extract (Amrani et al. 2008). Thus, both the resistance of poly(A) stimulation to disruption of the RNA backbone and sensitivity of stimulation to RNA length support the idea that the poly(A) tail promotes translation via a contact with the 5′ cap that is established through solution (Fig. 1A). Transcriptome-wide studies have shown that short mRNAs are also translated more efficiently in vivo (Arava et al. 2005; Lackner et al. 2007; Shah et al. 2013; Wang et al. 2013; Thompson and Gilbert 2017), and modeling has suggested that this is due to higher frequencies of initiation (Arava et al. 2005; Shah et al. 2013). Importantly, the association of the proteins forming the closed loop with mRNAs is not uniform across the transcriptome (Costello et al. 2015). The RNAs most strongly associated with the "closed-loop factors" are short (Thompson et al. 2016). Our results are consistent with these in vivo data and support the interpretation (Thompson and Gilbert 2017) that more efficient translation of shorter mRNAs reflects a more facile interaction between cap and poly(A) tail.

That the RNA backbone is not involved in poly(A)-dependent stimulation of translation is not surprising from a theoretical point of view: Any molecule tracking the RNA backbone would obviously collide with advancing ribosomes. If the closed loop were a stable structure, established once and for all before the RNA is first translated, the first round of translation would somehow have to be postponed until the closed loop is established. However, imaging of cellular polysomes by cryo-electron tomography (Brandt et al. 2010) or light microscopy (Adivarahan et al. 2018; Khong and Parker 2018) revealed mostly noncircular structures. (Note that the shortest RNA examined in the latter experiments was 5.5 kb long, and most RNAs were longer than 10 kb. Based on the discussion above, such RNAs would be less prone to forming end-to-end interactions.) Thus, the closed loop likely exists transiently as part of an association—dissociation equilibrium, that is, the interaction has to be reestablished multiple times throughout the lifetime of an mRNA. This would be

hard to reconcile with any end-to-end interaction mechanism making use of the RNA backbone. In summary, theoretical arguments and several types of experimental results suggest that the contact between the poly(A) tail and the 5′ end that facilitates translation initiation is established through solution.

As compared to poly(A)-dependent stimulation of translation, establishment of a repressed state due to factors bound to the 3′-UTR would be more easily compatible with a mechanism making use of the RNA backbone. However, repression of translation by SREs in the 3′-UTR also functioned in the face of a protein roadblock interrupting the RNA, even when this was coupled with an inverted 5′–3′ polarity of the regulatory sequences with respect to the ORF. The repressor complex formed on such chimeric RNAs was, by several criteria, equivalent to the one that forms on noninterrupted RNAs. As for poly(A)-dependent stimulation of translation, resistance of repression to a protein roadblock and to the inversion of 5′–3′ polarity rules out an establishment of the end-to-end interaction by mechanisms tracking the RNA backbone either by a helicase activity or by polymerization of a protein coat (Götze et al. 2017). However, with the same sets of mRNA molecules that uncovered the length-sensitivity of poly(A)-dependent stimulation, SRE-dependent repression worked equally well independently of RNA length. This unexpected discrepancy between length-sensitivity of poly(A)-dependent stimulation and insensitivity of SRE-dependent repression can be explained in two ways: The first explanation assumes that the 5′–3′ interactions responsible for translation repression are also established through solution but are more stable than the interactions responsible for translation stimulation. Increased RNA length decreases the effective concentration of the 5′ end with respect to the 3′ end. The extent to which such a decrease of the effective concentrations of the ends reduces the population of the end-to-end-associated state depends on the equilibrium dissociation constant of the end-to-end association; the associated state will be significantly populated if its dissociation constant is near or below the effective concentrations. Thus, the same increase in RNA length that reduces the 5′–3′ interaction responsible for poly(A)-dependent stimulation might have little effect on SRE-dependent repression if the repressive end-to-end interaction has a lower K_D. The absence of ribosome transit on the repressed RNAs likely also favors a more compact state (Adivarahan et al. 2018; Khong and Parker 2018), that is, a higher concentration of one end in the neighborhood of the other. The second explanation assumes that the mechanisms establishing 5′–3′ interactions responsible for SRE-dependent repression of translation are different from those responsible for poly(A)-dependent stimulation of translation. A hypothetical mechanism that reconciles the insensitivity of repression to both a protein roadblock and RNA length is depicted in Figure 1D: According to this hypothesis, components of the repressor complex can get hold of neighboring segments of the RNA without having to move along the backbone. This is likely to induce compaction of the RNA and may lead to inhibition of translation by sequestration of either the 5′ end or even the entire RNA. Such a model is attractive for several reasons: First, compaction of the RNA would be consistent with its observed rapid sedimentation (Fig. 6; Götze et al. 2017), which has also been observed for other repressed RNAs (Chekulaeva et al. 2006; Thermann and Hentze 2007). Second, the model would explain the observation that two components of the repressor complex, the DEAD-box helicase Me31B and its partner Trailer Hitch, bind the repressed RNA in multiple copies, roughly proportional to the length of the RNA (Ernoult-Lange et al. 2012; Götze et al. 2017). Third, a model for this hypothetical behavior of a component of the repressor complex is provided by the DEAD-box helicase Ded1. This enzyme can transfer from its initial binding site in ssDNA or RNA to a neighboring double-stranded nucleic acid with a link between the two provided by a streptavidin bridge, similar to the constructs used here (Yang and Jankowsky 2006). Fourth, the repression of *nanos* by Smaug binding to SREs is tight and kinetically stable, that is, apparently not part of a rapidly reversible association-dissociation equilibrium (Nelson et al. 2004; Jeske et al. 2011). In the context of embryo development, it seems desirable to reliably restrict the SRE effect to an intramolecular repression and prevent competing interactions with other mRNAs (Jeske et al. 2011). If the repressor complex did not immediately interact with the distant cap but engaged the entire RNA by contacting nearby RNA segments, SRE-dependent repression would presumably be relatively insensitive to competition by other mRNA molecules.

MATERIALS AND METHODS

Production and analysis of divalent streptavidin

His-tagged wild-type streptavidin and an untagged triple mutant inactive in biotin binding were separately expressed in *E. coli* as previously described (Howarth et al. 2006) (plasmids pET21a-Streptavidin-Alive; Addgene #20860; and pET21a-Streptavidin-Dead; Addgene #20859). Inclusion body pellets were dissolved in 6 M guanidinium hydrochloride (pH 1.5), and potentially contaminating biotin was removed by overnight dialysis against the same solvent. Concentrations of WT and mutant streptavidin were estimated by UV absorption and 20 mg of each subunit mixed in a 1:1 ratio. Protein was refolded and concentrated as in Schmidt and Skerra (1994). Soluble protein was loaded on a 15 ml Ni-NTA column (Qiagen) and eluted with a 60 ml gradient of 10 to 250 mM imidazole in 50 mM Tris-HCl, pH 7.8, 300 mM NaCl. The species containing two untagged subunits and, therefore, two biotin binding sites was identified from its relative elution position and its characteristic migration when loaded onto

an 8% SDS–polyacrylamide gel without boiling (Howarth et al. 2006). The concentration was determined by UV absorption.

The identity of divalent streptavidin was confirmed by native mass spectrometry: The buffer of divalent streptavidin and of commercial wild-type streptavidin (Promega) was exchanged to 200 mM ammonium acetate (7.5 M solution from Sigma-Aldrich [A2706]) with Amicon ultracentrifugal filters (30 kDa cut-off). The proteins were adjusted to 10 µM with 200 mM ammonium acetate. Aliquots were incubated for 30 min with a 10-fold excess of biotin, and samples with or without biotin were analyzed in a QToF II instrument (Waters). MassLynx software (Waters Micromass) was used for data evaluation. The observed mass of divalent streptavidin without biotin corresponded to the expectation (54,669 Da) (Howarth et al. 2006). Divalent streptavidin with two bound biotins has an expected mass of 55,157.6 Da; a mass of 55,158.7 Da was observed.

Transcription templates

Transcription templates for reporter RNAs were based on those described in Jeske et al. (2006). For the nLuc plasmids, the firefly luciferase (fLuc) ORF was removed by digestion with SacI and BglII and replaced by a PCR fragment with the NanoLuc ORF (nLuc; Promega). For the nLuc and fLuc RNAs, transcription templates were cut at a Pst1 site introduced, by mutagenesis, 30 nt downstream from the luciferase stop codon. This resulted in RNAs lacking both poly(A) and SREs. For the nLuc-p(A)N40 and fLuc-p(A)N40 RNAs, *nanos* sequences including the SREs were deleted by cutting with BglII and BamHI and religation. The sequence coding for MBP was amplified with flanking BamHI sites and cloned directly behind the stop codon of nLuc or fLuc in the BglII site of the plasmids. The second MBP sequence was cloned into the existing BglII site of the first MBP sequence. Variants of the fLuc-MBP-SRE$^{\pm}$ and fLuc-MBP-SRE$^{\pm}$-poly(A) constructs were made by site-specific mutagenesis converting the fLuc stop codon to a glutamate codon. As a result, the fLuc ORF was joined to that of MBP with an arginine-serin linker. Upon digestion of the DNA templates described with BamHI or KpnI, transcription resulted in RNAs lacking poly(A) or carrying an internal A_{60} sequence followed by 40 residues of mixed sequence.

Templates for regulatory RNAs containing both SREs and a poly(A) stretch were generated by amplification, from the nLuc-SRE-p(A)N40 plasmid, of the sequences starting after the nLuc stop codon and ending at the end of the N40 sequence. The PCR product was cloned into a pBlueskript SK vector digested with SacI and KpnI. For the synthesis of regulatory RNAs lacking SREs, the corresponding template sequences were removed by digestion, with Eco53kI and BamHI, of the vector for the complete regulatory RNA. The BamHI overhang was filled in by Klenow DNA polymerase, and the vector was religated. The fLuc reporter RNA of Jeske et al. (2006) was used as the long regulatory RNA depicted in Figure 3A. All newly created transcription templates were checked by DNA sequencing.

Synthesis and biotinylation of RNA

For the synthesis of 5′-biotinylated regulatory RNAs, a 5′ biotin-ApG initiator nucleotide was incorporated cotranscriptionally (Pitulle et al. 1992). A 25 µL transcription reaction contained 1x transcription buffer (Ambion), 30 mM DTT, 10 mM $MgCl_2$, 0.01 U pyrophosphatase (Thermo Fisher), 20 U RNasin (Promega), 1 µg linearized plasmid, 1.5 mM 5′ biotin-ApG (Jena Bioscience), 1.5 mM ATP and CTP, 1 mM UTP, 20 µCi α-^{32}P UTP, and 100 U T3 RNA polymerase (NEB). Reactions were started by addition of 0.15 mM GTP. After 1 h at 37°C, 0.15 mM GTP was again added, and the reactions were further incubated for 3 h.

For the synthesis of 3′-biotinylated regulatory RNAs, transcription reactions were as above except that 5′ biotin-ApG was replaced by 7 mM A-cap (Jena Bioscience), and GTP, ATP, and CTP were all used at 3 mM. After transcription, samples were digested with 10 U DNase I (Roche), followed by a Sephadex-G50 spin column purification, phenol–chloroform-extraction and ethanol precipitation. The purified RNAs were heated to 95°C for 5 min and chilled on ice. A 25 µL biotinylation reaction contained 1× T4 RNA ligase buffer (NEB), 1 µM RNA, 2 µM biotin-pCp (Jena Bioscience), 10% DMSO, 16% (w/v) PEG-8000, 1 mM ATP, 32.5 U RNasin (Promega), and 50 U T4-RNA ligase I (NEB) and was incubated for 16 h at 6°C.

For 3′-biotinylated nLuc RNAs, 7 mM anti-reverse cap analog (NEB) was used during transcription. Biotinylation was carried out by ligation as above.

With the exception of the long fLuc-SRE-p(A) regulatory RNA, all RNAs used to generate chimeras were gel-purified. They were quantified from the amount of radioactivity incorporated and the known specific activity of UTP.

Uninterrupted mRNAs were synthesized like the nLuc RNAs to be used for 3′ biotinylation except that the UTP concentration was 3 mM and no radioactive nucleotide was added. RNAs were purified by Sephadex G50 spin columns and ethanol-precipitated from 2.5 M ammonium acetate. Their concentrations were determined from their UV absorbance.

Assembly of chimeric reporter constructs

Chimeric constructs were assembled at room temperature: 50 µL oligo-$(dT)_{25}$ magnetic beads (NEB) were equilibrated in a protein LoBind tube (Eppendorf) with binding buffer (20 mM Tris-HCl, pH 7.5, 500 mM LiCl, 0.5% lithium dodecylsulfate, 1 mM EDTA, 5 mM DTT, 0.1 g/L methylated BSA [Means and Feeney 1968], 0.1 g/L *E. coli* rRNA [Roche]) for 30 min. After removal of the buffer, 2.5 pmol regulatory RNA in 100 µL binding buffer was incubated with the beads for 5 min. Thirty picomoles divalent streptavidin in 100 µL of a 1:1 mixture of binding buffer and low-salt buffer (20 mM Tris-HCl, pH 7.5, 200 mM LiCl, 1 mM EDTA, 0.1 g/L methylated BSA, 0.1 g/L *E. coli* rRNA) was added and incubated for 45 min. The beads were washed once with 200 µL wash buffer (as binding buffer, but lacking lithium dodecylsulfate and DTT), transferred to a DNA LoBind tube (Eppendorf) and washed twice with 200 µL low-salt buffer. Three picomoles of nLuc RNA in 100 µL low-salt buffer was added and incubated for 60 min. The beads were washed once with 200 µL wash buffer and twice with 200 µL low-salt buffer. Chimeric constructs were eluted at 50°C for 2 min in 50 µL 10 mM Tris-HCl, pH 7.5. The assembly of chimeric RNAs was checked by electrophoresis in 5% polyacrylamide gels in 1× TBE buffer at 4°C. Aliquots of the chimeric RNAs were loaded in formamide loading buffer with or without boiling. ImageQuant 5.2 was used for quantification.

Embryo extract, in vitro translation, and related assays

Drosophila embryo extract was prepared and in vitro translation of luciferase reporter RNAs performed as previously described (Götze et al. 2017). As controls, RNAs were translated in untreated rabbit reticulocyte lysate (RRL; Promega). Each reaction contained 0.2 nM chimeric or 2 nM uninterrupted mRNA, 30% RRL, 79 mM potassium acetate, 0.5 mM magnesium acetate, 20 mM creatine phosphate, 0.08 g/L rabbit muscle creatine kinase (Sigma), 20 µM amino acid mix, 0.05 g/L yeast tRNA, 0.2 g/L short RNA (Götze et al. 2017). The reactions were incubated at 30°C for 30 min. Nano-Glo and One-Glo reagents (Promega) were used for nLuc and fLuc activity assays, respectively. Each translation experiment in embryo extract was carried out three times in parallel; that is, $n = 3$ reflects nine reactions. Experiments in RRL were carried out twice in parallel. Statistical significance of poly(A)-dependent stimulation and SRE-dependent repression of translation was evaluated by the two-tailed *t*-test. The calculation was performed for each independent experiment on the basis of three technical replicates, and all *P*-values obtained for one type of RNA were averaged.

RNase protection assays were performed as previously described (Götze et al. 2017), except that 0.2 nM RNA and 0.17 U/µL RNase I_f were used. Sucrose density gradient centrifugation was performed with 0.2 nM RNA as previously described (Götze et al. 2017).

RNA stability assays

Fifteen femtomoles of chimeric constructs was incubated with *Drosophila* embryo extract under translation conditions in a volume of 15 µL. Either immediately or after 30 min at 25°C, 20 µL oligo-$(dT)_{25}$ magnetic beads (NEB) were added, and the volume was increased to 100 µL with binding buffer (as described for assembly of chimeras). After 5 min at 25°C, the supernatant was removed, and the beads were washed once with binding buffer. The constructs were eluted with 100 µL water for 2 min at 50°C and treated with 20 µg proteinase K in 1× PK buffer (100 mM Tris-HCl pH 7.9, 150 mM NaCl, 12.5 mM EDTA, 1% SDS) for 30 min at 37°C. RNAs were ethanol-precipitated, dissolved in loading buffer containing 80% formamide, boiled, and loaded onto a 5% denaturing polyacrylamide gel.

One picomole uninterrupted RNA was incubated in a 25 µL reaction under preincubation conditions in *Drosophila* embryo extract. After 0 or 30 min, 10 µL aliquots of the reaction were mixed with 10 µL 2× PK buffer containing 20 µg proteinase K and incubated for 30 min at 37°C. RNAs were ethanol-precipitated, dissolved in RNA-loading-buffer (Thermo Scientific), and resolved on denaturing agarose gels containing 1× MOPS buffer and 2.2 M formaldehyde (Sambrook and Russell 2001). RNAs were detected by northern blotting with 5′-labeled synthetic DNA oligonucleotide probes. Image Quant 5.2 was used for quantification.

SUPPLEMENTAL MATERIAL

Supplemental material is available for this article.

ACKNOWLEDGMENTS

We are grateful to Christian Ihling and Christian Arlt for MS analysis of strepavidin; to Moritz Schmidt for cloning nLuc; to Christiane Rammelt for advice and helpful discussions; to Filip Pekovic for sharing embryo extract; to Bodo Moritz for initial experiments in this project; and to Mandy Jeske and Nancy Standart for critical comments on an earlier version of the manuscript. This work was supported by grants from the DFG to E.W. (GRK 1591 and WA548/16-1).

Received October 23, 2019; accepted February 24, 2020.

REFERENCES

Adivarahan S, Livingston N, Nicholson B, Rahman S, Wu B, Rissland OS, Zenklusen D. 2018. Spatial organization of single mRNPs at different stages of the gene expression pathway. *Mol Cell* **72:** 727–738. doi:10.1016/j.molcel.2018.10.010

Amrani N, Ghosh S, Mangus DA, Jacobson A. 2008. Translation factors promote the formation of two states of the closed-loop mRNP. *Nature* **453:** 1276–1285. doi:10.1038/nature06974

Arava Y, Boas FE, Brown PO, Herschlag D. 2005. Dissecting eukaryotic translation and its control by ribosome density mapping. *Nucleic Acids Res* **33:** 2421–2432. doi:10.1093/nar/gki331

Bashirullah A, Halsell SR, Cooperstock RL, Kloc M, Karaiskakis A, Fisher WW, Fu W, Hamilton JK, Etkin LD, Lipshitz HD. 1999. Joint action of two RNA degradation pathways controls the timing of maternal transcript elimination at the midblastula transition in *Drosophila melanogaster*. *EMBO J* **18:** 2610–2620. doi:10.1093/emboj/18.9.2610

Bergsten SE, Gavis ER. 1999. Role for mRNA localization in translational activation but not spatial restriction of nanos RNA. *Development* **126:** 659–669.

Bienroth S, Wahle E, Suter-Crazzolara C, Keller W. 1991. Purification and characterisation of the cleavage and polyadenylation specificity factor involved in the 3′ processing of messenger RNA precursors. *J Biol Chem* **266:** 19768–19776.

Bönisch C, Temme C, Moritz B, Wahle E. 2007. Degradation of *hsp70* and other mRNAs in *Drosophila* via the 5′–3′ pathway and its regulation by heat shock. *J Biol Chem* **282:** 21818–21828. doi:10.1074/jbc.M702998200

Brandt F, Carlson LA, Hartl FU, Baumeister W, Grunewald K. 2010. The three-dimensional organization of polyribosomes in intact human cells. *Mol Cell* **39:** 560–569. doi:10.1016/j.molcel.2010.08.003

Charenton C, Gaudon-Plesse C, Fourati Z, Taverniti V, Back R, Kolesnikova O, Seraphin B, Graille M. 2017. A unique surface on Pat1 C-terminal domain directly interacts with Dcp2 decapping enzyme and Xrn1 5′–3′ mRNA exonuclease in yeast. *Proc Natl Acad Sci* **114:** E9493–E9501. doi:10.1073/pnas.1711680114

Chekulaeva M, Hentze MW, Ephrussi A. 2006. Bruno acts as a dual repressor of *oskar* translation, promoting mRNA oligomerization and formation of silencing particles. *Cell* **124:** 521–533. doi:10.1016/j.cell.2006.01.031

Colegrove-Otero LJ, Minshall N, Standart N. 2005. RNA-binding proteins in early development. *Crit Rev Biochem Mol Biol* **40:** 21–73. doi:10.1080/10409230590918612

Coller JM, Gray NK, Wickens MP. 1998. mRNA stabilization by poly(A) binding protein is independent of poly(A) and requires translation. *Genes Dev* **12:** 3226–3235. doi:10.1101/gad.12.20.3226

Costello J, Castelli LM, Rowe W, Kershaw CJ, Talavera D, Mohammad-Qureshi SS, Sims PFG, Grant CM, Pavitt GD, Hubbard SJ, et al. 2015. Global mRNA selection mechanisms for translation initiation. *Genome Biol* **16:** 10. doi:10.1186/s13059-014-0559-z

Couttet P, Fromont-Racine M, Steel D, Pictet R, Grange T. 1997. Messenger RNA deadenylylation precedes decapping in mammalian cells. *Proc Natl Acad Sci* **94:** 5628–5633. doi:10.1073/pnas.94.11.5628

Dahanukar A, Wharton RP. 1996. The Nanos gradient in *Drosophila* embryos is generated by translational regulation. *Genes Dev* **10:** 2610–2620. doi:10.1101/gad.10.20.2610

Dahanukar A, Walker JA, Wharton RP. 1999. Smaug, a novel RNA-binding protein that operates a translational switch in *Drosophila*. *Mol Cell* **4:** 209–218. doi:10.1016/S1097-2765(00)80368-8

Decker CJ, Parker R. 1993. A turnover pathway for both stable and unstable mRNAs in yeast: evidence for a requirement for deadenylation. *Genes Dev* **7:** 1632–1643. doi:10.1101/gad.7.8.1632

Dugaiczyk A, Boyer HW, Goodman HM. 1975. Ligation of EcoRI endonuclease-generated DNA fragments into linear and circular structures. *J Mol Biol* **96:** 171–184. doi:10.1016/0022-2836(75)90189-8

Ephrussi A, Lehmann R. 1992. Induction of germ cell formation by *oskar*. *Nature* **358:** 387–392. doi:10.1038/358387a0

Ernoult-Lange M, Baconnais S, Harper M, Minshall N, Souquere S, Boudier T, Benard M, Andrey P, Pierron G, Kress M, et al. 2012. Multiple binding of repressed mRNAs by the P-body protein Rck/p54. *RNA* **18:** 1702–1715. doi:10.1261/rna.034314.112

Gallie DR. 1991. The cap and poly(A) tail function synergistically to regulate mRNA translational efficiency. *Genes Dev* **5:** 2108–2116. doi:10.1101/gad.5.11.2108

Gavis ER, Lehmann R. 1992. Localization of nanos RNA controls embryonic polarity. *Cell* **71:** 301–313. doi:10.1016/0092-8674(92)90358-J

Gavis ER, Lehmann R. 1994. Translational regulation of nanos by RNA localization. *Nature* **369:** 315–318. doi:10.1038/369315a0

Götze M, Dufourt J, Ihling C, Rammelt C, Pierson S, Ambrani N, Temme C, Sinz A, Simonelig M, Wahle E. 2017. Translational repression of the *Drosophila nanos* mRNA involves the RNA helicase Belle and RNA coating by Me31B and Trailer hitch. *RNA* **24:** 1721–1737.

Gray NK, Coller JM, Dickson KS, Wickens MP. 2000. Multiple portions of poly(A)-binding protein stimulate translation in vivo. *EMBO J* **19:** 4723–4733. doi:10.1093/emboj/19.17.4723

Guo JU, Bartel DP. 2016. RNA G-quadruplexes are globally unfolded in eukaryotic cells and depleted in bacteria. *Science* **353:** aaf571. doi:10.1126/science.aaf4924

Howarth M, Chinnapen DJF, Gerrow K, Dorrestein PC, Grandy MR, Kelleher NL, El-Husseini A, Ting AY. 2006. A monovalent streptavidin with a single femtomolar biotin binding site. *Nat Methods* **3:** 267–273. doi:10.1038/nmeth861

Iizuka N, Najita L, Franzusoff A, Sarnow P. 1994. Cap-dependent and cap-independent translation by internal initiation of messenger-RNAs in cell-extracts prepared from *Saccharomyces cerevisiae*. *Mol Cell Biol* **14:** 7322–7330. doi:10.1128/MCB.14.11.7322

Imataka H, Gradi A, Sonenberg N. 1998. A newly identified N-terminal amino acid sequence of human eIF4G binds poly(A)-binding protein and functions in poly(A)-dependent translation. *EMBO J* **17:** 7480–7489. doi:10.1093/emboj/17.24.7480

Jacobson A. 1996. Poly(A) metabolism and translation: the closed-loop model. In *Translation control* (ed. Hershey JWB, et al.), pp. 451–480. Cold Spring Harbor Laboratory Press, Cold Spring Harbor, NY.

Jeske M, Meyer S, Temme C, Freudenreich D, Wahle E. 2006. Rapid ATP-dependent deadenylation of nanos mRNA in a cell-free system from *Drosophila* embryos. *J Biol Chem* **281:** 25124–25133. doi:10.1074/jbc.M604802200

Jeske M, Moritz B, Anders A, Wahle E. 2011. Smaug assembles an ATP-dependent stable complex repressing nanos mRNA translation at multiple levels. *EMBO J* **30:** 90–103. doi:10.1038/emboj.2010.283

Jonas S, Izaurralde E. 2015. Towards a molecular understanding of microRNA-mediated gene silencing. *Nat Rev Genet* **16:** 421–433. doi:10.1038/nrg3965

Kahvejian A, Svitkin YV, Sukarieh R, M'Boutchou MN, Sonenberg N. 2005. Mammalian poly(A)-binding protein is a eukaryotic translation initiation factor, which acts via multiple mechanisms. *Genes Dev* **19:** 104–113. doi:10.1101/gad.1262905

Kalifa Y, Huang T, Rosen LN, Chatterjee S, Gavis ER. 2006. Glorund, a *Drosophila* hnRNP F/H homolog, is an ovarian repressor of *nanos* translation. *Dev Cell* **10:** 291–301. doi:10.1016/j.devcel.2006.01.001

Khong A, Parker R. 2018. mRNP architecture in translating and stress conditions reveals an ordered pathway of mRNP compaction. *J Cell Biol* **217:** 4124–4140. doi:10.1083/jcb.201806183

Kühn U, Wahle E. 2004. Structure and function of poly(A) binding proteins. *Biochim Biophys Acta* **1678:** 67–84. doi:10.1016/j.bbaexp.2004.03.008

Lackner DH, Beilharz TH, Marguerat S, Mata J, Watt S, Schubert F, Preiss T, Bähler J. 2007. A network of multiple regulatory layers shapes gene expression in fission yeast. *Mol Cell* **26:** 145–155. doi:10.1016/j.molcel.2007.03.002

Lai WJC, Kayedkhordeh M, Cornell EV, Farah E, Bellaousov S, Rietmeijer R, Salsi E, Mathews DH, Ermolenko DN. 2018. mRNAs and lncRNAs intrinsically form secondary structures with short end-to-end distances. *Nat Commun* **9:** 4328. doi:10.1038/s41467-018-06792-z

Leija-Martínez N, Casas-Flores S, Cadena-Nava RD, Roca JA, Mendez-Cabanas JA, Gomez E, Ruiz-Garcia J. 2014. The separation between the 5′–3′ ends in long RNA molecules is short and nearly constant. *Nucleic Acids Res* **42:** 13963–13968. doi:10.1093/nar/gku1249

Ling SHM, Qamra R, Song HW. 2011. Structural and functional insights into eukaryotic mRNA decapping. *WIRES RNA* **2:** 193–208. doi:10.1002/wrna.44

Lingelbach K, Dobberstein B. 1988. An extended RNA/RNA duplex structure within the coding region of mRNA does not block translational elongation. *Nucleic Acids Res* **16:** 3405–3414. doi:10.1093/nar/16.8.3405

Means GE, Feeney RE. 1968. Reductive alkylation of amino groups in proteins. *Biochemistry* **7:** 2192–2201. doi:10.1021/bi00846a023

Munroe D, Jacobson A. 1990. Messenger-RNA poly(A) tail, a 3′ enhancer of translational initiation. *Mol Cell Biol* **10:** 3441–3455. doi:10.1128/MCB.10.7.3441

Nelson MR, Leidal AM, Smibert CA. 2004. *Drosophila* Cup is an eIF4E-binding protein that functions in Smaug-mediated translational repression. *EMBO J* **23:** 150–159. doi:10.1038/sj.emboj.7600026

Park EH, Walker SE, Lee JM, Rothenburg S, Lorsch JR, Hinnebusch AG. 2011. Multiple elements in the eIF4G1 N-terminus promote assembly of eIF4G1•PABP mRNPs in vivo. *EMBO J* **30:** 302–316. doi:10.1038/emboj.2010.312

Piron M, Vende P, Cohen J, Poncet D. 1998. Rotavirus RNA-binding protein NSP3 interacts with eIF4GI and evicts the poly(A) binding protein from eIF4. *EMBO J* **17:** 5811–5821. doi:10.1093/emboj/17.19.5811

Pitulle C, Kleineidam RG, Sproat B, Krupp G. 1992. Initiator oligonucleotides for the combination of chemical and enzymatic RNA-synthesis. *Gene* **112:** 101–105. doi:10.1016/0378-1119(92)90309-D

Sambrook J, Russell DW. 2001. Separation of RNA according to size: electrophoresis of RNA through agarose gels containing formaldehyde. In *Molecular cloning: a laboratory manual*, 3rd ed., Vol. 1. Cold Spring Harbor Laboratory Press, Cold Spring Harbor, New York.

Schmidt TGM, Skerra A. 1994. One-step affinity purification of bacterially produced proteins by means of the strep tag and immobilized recombinant core streptavidin. *J Chromatogr A* **676:** 337–345. doi:10.1016/0021-9673(94)80434-6

Schwartz DC, Parker R. 2000. mRNA decapping in yeast requires dissociation of the cap binding protein, eukaryotic translation initiation factor 4E. *Mol Cell Biol* **20:** 7033–7942. doi:10.1128/MCB.20.21.7933-7942.2000

Semotok JL, Cooperstock RL, Pinder BD, Vari HK, Lipshitz HD, Smibert CA. 2005. Smaug recruits the CCR4/POP2/NOT deadenylase complex to trigger maternal transcript localization in the early *Drosophila* embryo. *Curr Biol* **15:** 284–294. doi:10.1016/j.cub.2005.01.048

Shah P, Ding Y, Niemczyk M, Kudla G, Plotkin JB. 2013. Rate-limiting steps in yeast protein translation. *Cell* **153:** 1589–1601. doi:10.1016/j.cell.2013.05.049

Sharif H, Conti E. 2013. Architecture of the Lsm1-7-Pat1 complex: a conserved assembly in eukaryotic mRNA turnover. *Cell Rep* **5:** 283–291. doi:10.1016/j.celrep.2013.10.004

Sheets MD, Wu M, Wickens M. 1995. Polyadenylation of c-*mos* mRNA as a control point in *Xenopus* meiotic maturation. *Nature* **374:** 511–516. doi:10.1038/374511a0

Smibert CA, Wilson JE, Kerr K, Macdonald PM. 1996. Smaug protein represses translation of unlocalized nanos mRNA in the *Drosophila* embryo. *Genes Dev* **10:** 2600–2609. doi:10.1101/gad.10.20.2600

Smibert CA, Lie YS, Shillinglaw W, Henzel WJ, Macdonald PM. 1999. Smaug, a novel and conserved protein, contributes to repression of nanos mRNA translation in vitro. *RNA* **5:** 1535–1547. doi:10.1017/S1355838299991392

Smith JL, Wilson JE, Macdonald PM. 1992. Overexpression of *oskar* directs ectopic activation of *nanos* and presumptive pole cell-formation in *Drosophila* embryos. *Cell* **70:** 849–859. doi:10.1016/0092-8674(92)90318-7

Takyar S, Hickerson RP, Noller HF. 2005. mRNA helicase activity of the ribosome. *Cell* **120:** 49–58. doi:10.1016/j.cell.2004.11.042

Tamayo JV, Teramoto T, Chatterjee S, Hall TMT, Gavis ER. 2017. The *Drosophila* hnRNP F/H homolog glorund uses two distinct RNA-binding modes to diversify target recognition. *Cell Rep* **19:** 150–161. doi:10.1016/j.celrep.2017.03.022

Tarun SZ, Sachs AB. 1995. A common function for mRNA-5′ and mRNA-3′ ends in translation initiation in yeast. *Gene Dev* **9:** 2997–3007. doi:10.1101/gad.9.23.2997

Tarun SZ, Sachs AB. 1996. Association of the yeast poly(A) tail binding protein with translation initiation factor eIF-4G. *EMBO J* **15:** 7168–7177. doi:10.1002/j.1460-2075.1996.tb01108.x

Thermann R, Hentze MW. 2007. *Drosophila* miR2 induces pseudo-polysomes and inhibits translation initiation. *Nature* **447:** 875–878. doi:10.1038/nature05878

Thompson MK, Gilbert WV. 2017. mRNA length-sensing in eukaryotic translation: reconsidering the "closed loop" and its implications for translational control. *Curr Genet* **63:** 613–620. doi:10.1007/s00294-016-0674-3

Thompson MK, Rojas-Duran MF, Gangaramani P, Gilbert WV. 2016. The ribosomal protein Asc1/RACK1 is required for efficient translation of short mRNAs. *Elife* **5:** e11154. doi:10.7554/eLife.11154

Vicens Q, Kieft JS, Rissland OS. 2018. Revisiting the closed-loop model and the nature of mRNA 5′–3′ communication. *Mol Cell* **72:** 805–812. doi:10.1016/j.molcel.2018.10.047

Wang JC, Davidson N. 1966. On the probability of ring closure of λ DNA. *J Mol Biol* **19:** 469–482. doi:10.1016/S0022-2836(66)80017-7

Wang C, Lehmann R. 1991. Nanos is the localized posterior determinant in *Drosophila*. *Cell* **66:** 637–647. doi:10.1016/0092-8674(91)90110-K

Wang T, Cui YZ, Jin JJ, Guo JH, Wang GB, Yin XF, He QY, Zhang G. 2013. Translating mRNAs strongly correlate to proteins in a multivariate manner and their translation ratios are phenotype specific. *Nucleic Acids Res* **41:** 4743–4754. doi:10.1093/nar/gkt178

Wells SE, Hillner PE, Vale RD, Sachs AB. 1998. Circularization of mRNA by eukaryotic translation initiation factors. *Mol Cell* **2:** 135–140. doi:10.1016/S1097-2765(00)80122-7

Wickens M, Goodwin EB, Kimble J, Strickland S, Hentze M. 2000. Translational control of developmental decisions. In *Translational control of gene expression* (ed. Sonenberg N, et al.). Cold Spring Harbor Laboratory Press, Cold Spring Harbor, New York.

Yang QS, Jankowsky E. 2006. The DEAD-box protein Ded1 unwinds RNA duplexes by a mode distinct from translocating helicases. *Nat Struct Mol Biol* **13:** 981–986. doi:10.1038/nsmb1165

Yoffe AM, Prinsen P, Gelbart WM, Ben-Shaul A. 2011. The ends of a large RNA molecule are necessarily close. *Nucleic Acids Res* **39:** 292–299. doi:10.1093/nar/gkq642

Zaessinger S, Busseau I, Simonelig M. 2006. Oskar allows *nanos* mRNA translation in *Drosophila* embryos by preventing its deadenylation by Smaug/CCR4. *Development* **133:** 4573–4583. doi:10.1242/dev.02649